Research Report 19

OCTOBER, 1956

Radiation Measurements on the Greenland Ice Cap

SNOW, ICE AND PERMAFROST
RESEARCH ESTABLISHMENT
Corps of Engineers, U. S. Army

SIPRE Report 19

RADIATION MEASUREMENTS ON THE GREENLAND ICE CAP

by M. Diamond and R. W. Gerdel

This report presents the results obtained from a portion of the studies made by SIPRE at the Site 2 Greenland test area during the summer of 1955. These investigations, conducted under Corps of Engineers Greenland Project 23, *Snow drift, white-out and radiation studies*, were undertaken as a part of SIPRE Project 22.5-3, *Radiational and convective heat transfer between the atmosphere and the terrain.*

Messrs. W. H. Parrott, R. G. Baughman, and K. J. Walsh, SIPRE employees assigned to Greenland Project 23 for the summer of 1955, assisted in conducting the studies.

Department of the Army Project 8-66-02-004

RADIATION MEASUREMENTS ON THE GREENLAND ICE CAP

by
M. Diamond and R. W. Gerdel

ABSTRACT

Measurements were made of global and net radiation between 6 July and 7 August 1955 at a site on the Greenland Ice Cap located near 78° N. latitude and at an elevation of 6800 ft. Snow-surface temperatures during this period were below 0 C and mean cloudiness was 0.7. Total incident global radiation measured during the 33-day period amounted to 20, 628 *ly*, of which only 3059 *ly*, or about 15%, were absorbed by the snow cover. Most of the absorbed global radiation was re-emitted as long-wave radiation, so the net gain during the observation period amounted to not more than 7.6 *ly*/day.

Diffuse sky radiation amounted to only 19% of all incoming global radiation measured at the ice-cap research site. In the temperate zone, diffuse sky radiation amounts to 30% or more of the incoming radiation. The small amount of diffuse sky radiation indicates low atmospheric turbidity in this polar climatic zone.

Incident global radiation was reduced by 6% in the presence of a 0.5 cloud cover. Under full overcast conditions the snow surface received 65% of the global radiation measured on clear days. In the temperate zone as little as 30% of global radiation reaches the earth under full cloud cover. The large amount of global radiation received in the Arctic under full cloud cover is the primary cause of one form of arctic white-out. Accompanying the small decrease in global radiation caused by cloudiness is a large decrease in effective outgoing long-wave radiation, with an increase in the net radiation balance. This condition contributes to a greater potential ablation of the snow and ice cover during cloudy seasons.

The long-wave radiation balance at this site on the ice cap was always negative during the period covered by this study.

Errors associated with the measurement of solar radiation at the low sun angles which prevailed at the research site were found to be about –3%. No correction was applied to the basic data, however, since there were insufficient data to establish the consistency of this error over the period of observation.

During periods of blowing and drifting snow, 6% more global radiation was measured at 1.25 m above the snow surface than at 5.7 m elevation. The increase may be due to multiple reflection within the layer of blowing snow.

The atmospheric transmission coefficient at the ice-cap site was found to be 0.968. This high value was associated with the low atmospheric turbidity.

The heat balance of the snow cover as computed from the radiation measurements and a temperature profile in the snow was found to be 7.6 *ly*/day at the ice-cap site. This is a negligible heat gain when compared with the 400 *ly*/day gain by a spring snow pack in the Sierra Nevada of California. For the entire season when the sun is above the horizon, the estimated net gain by the ice cap is 1000 *ly*, no more than a 2-1/2-day heat supply used in melting the snow of the High Sierra.

Some measurements made with a silicon solar battery similar to those developed by the Bell Telephone Laboratories indicate that it may have a significantly higher efficiency on the ice cap than in the more temperate zone. Verification of this apparent increase in efficiency and the causes for it require further study of the performance of the p-n junction cells in the Arctic.

CONTENTS

I. INTRODUCTION

1. North of 75° the sun is continuously above the horizon from the first of May to the last of August. In June and July the Arctic has a potentially greater supply of solar radiation than any other area in the world. The reflection of radiation from the snow and ice cover, which may amount to more than 85% of the incident radiation, decreases the solar energy available for melting, thus aiding in the perpetuation of the extensive ice caps and snow fields. On the other hand the large amount of reflected radiation may provide an additional supply of thermal energy for applied use in the Arctic.

Any efforts to apply a heat budget balance to the problem of distribution, accretion, and ablation of the snow cover, ice caps, or glaciers require quantitative information on solar and terrestrial radiation. Reliable information on available solar radiation is also needed as a basis for determining the applicability to the Arctic of some of the promising recent developments in applied use of solar energy.

The high ice cap in north-central Greenland provides an almost ideal Arctic site for radiation measurements during the summer months. The level snow surface extends circumferentially to the horizon. The almost constant wind movement of snow maintains a surface with a high albedo. The persistent low temperature and absence of melting at this location eliminates some of the problems associated with the measurement of radiation and the derivation of a radiation heat budget in a more temperate climate. These advantageous conditions were utilized during the summer of 1955 to obtain a series of radiation measurements which provided information on the following parameters.

a. Global radiation (combined solar and diffused sky radiation) on a horizontal surface.
b. Global radiation hemispherically reflected from the snow surface (albedo).
c. Diffuse sky radiation with the solar disk occulted.
d. Incident solar radiation on a surface normal to the sun.
e. Total incoming global plus long-wave radiation in approximately the 0.3 μ to 300 μ range.
f. Net (incoming or outgoing) all-wave radiation in the 0.3 μ to 300 μ range.
g. Attenuation of the global radiation by blowing or falling snow or by the several forms of white-out to an elevation of 5.7 m above the snow surface.

In addition, measurements and observations permitted evaluation of: the effect of cloud cover on global and long-wave radiation balances over a continuous snow cover; the response of the pyrheliometers at low sun angles; the transmission coefficient of the atmosphere above the high ice cap; and the heat balance of the snow cover at this site for a brief period near the summer solstice.

II. INSTRUMENTATION

2. Instruments and recorders were installed for the summer at a permanent military station located on the Greenland Ice Cap approximately 200 miles east of Thule, near 78° N. latitude. The elevation of this station is about 6800 ft. A lightweight tubular aluminum tower about 8 m high was erected to support meteorological equipment, including some of the radiation-measuring instruments used in this study. Other radiometers and pyrheliometers were mounted on 4-ft-high supports in the vicinity of the tower. A reliable 110-v a-c power supply was available at this site for the operation of the high-speed potentiometer-type recorders which were used in these studies.

Incident global radiation was measured with a 10-junction Eppley hemispherical pyrheliometer mounted with the thermopile target facing the zenith.

Reflected global radiation was measured with a 10-junction Eppley hemispherical

pyrheliometer mounted with the thermopile target facing, and in plane parallel with, the snow surface.

Normal incident radiation was measured with an Eppley normal incident pyrheliometer installed on a manually operated altitude-azimuth mount which permitted adjustment of the thermopile target normal to the solar disk each time a measurement was made.

Diffuse sky radiation was obtained at appropriate intervals by momentarily occulting the sun so the target of the pyrheliometer used for global radiation measurements received no direct solar radiation.

Incoming all-wave radiation, consisting of global radiation and long-wave radiation, was measured with an aspirated Gier-Dunkle total radiometer.

Net all-wave radiation, which is the difference between the total incoming global and long-wave radiation and the total reflected global and outgoing long-wave radiation, was measured with an aspirated Gier-Dunkle net hemispherical radiometer.

The global radiation gradient was measured during periods of blowing snow and arctic white-outs with Eppley pyrheliometers mounted at 1.25, 3.5, and 5.7 m above the snow surface.

Recording of data.

3. The hemispherical pyrheliometers used for incident global and reflected radiation measurements and the total and net radiometers used for all-wave radiation measurements were connected to recording potentiometers to provide a continuous strip chart record. Measurements with the normal incident pyrheliometer were made several times each day using a manually operated potentiometer. When global radiation gradient records were required, an automatic step-switching system was used to provide a 1-min record on the strip chart recorder for the pyrheliometers mounted at each of the three elevations.

In addition, the output of a silicon solar energy converter (solar battery) was measured at intervals with a portable milliammeter.

Photographs of the installation at the ice-cap research site are shown in Figures 1, 2, and 3.

III. RESULTS

4. Incident and reflected global radiation and net all-wave radiation obtained during the course of these studies, as tabulated from the recorder charts, are included as an appendix to this report. These data served as the basis for the development of those sections of this report which deal with specific phases of the radiation investigations.

Global radiation.

5. The total daily incoming global radiation and the amount absorbed by the snow surface, computed from the difference between the incident and reflected global radiation, are plotted in Figure 4. For comparison purposes the mean daily cloud cover is included in this figure. The total global radiation incident on the snow surface from 6 July to 7 August inclusive was 20,628 *ly*,*

* 1 langley (*ly*) = 1 cal/cm^2.

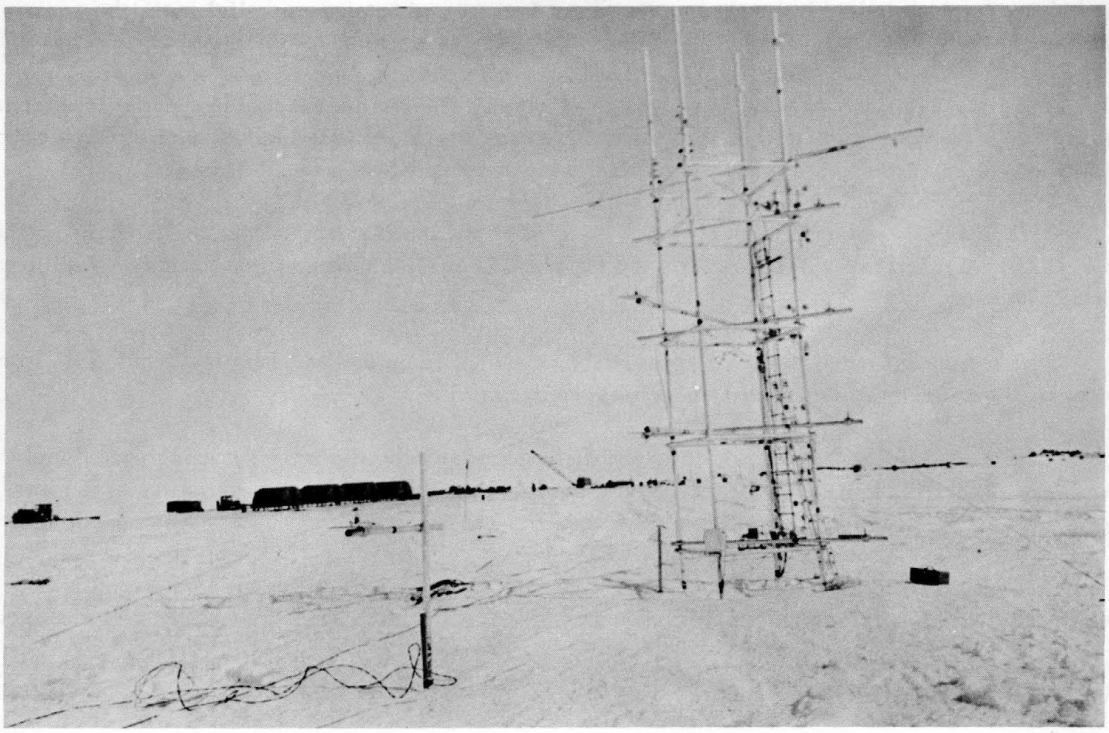

Figure 1. Meteorological instrumentation at Site 2 where the radiation measurements were made.

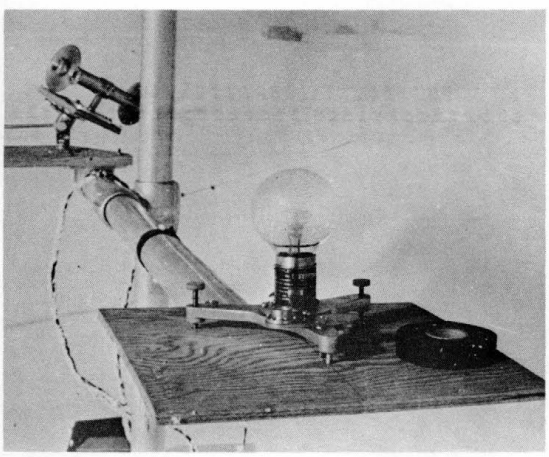

Figure 2. One of the Eppley total hemispherical pyrheliometers (foreground) and the Eppley normal incident pyrheliometer (background), shown as installed at the ice-cap site.

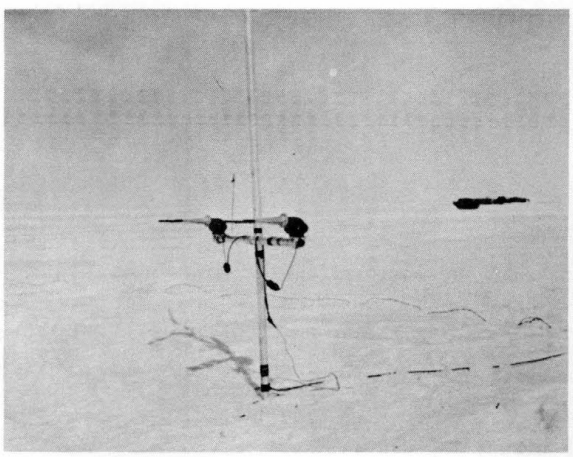

Figure 3. Gier-Dunkle radiometers for hemispherical measurement of total incoming all-wave radiation and net all-wave radiation, as installed at the ice-cap site.

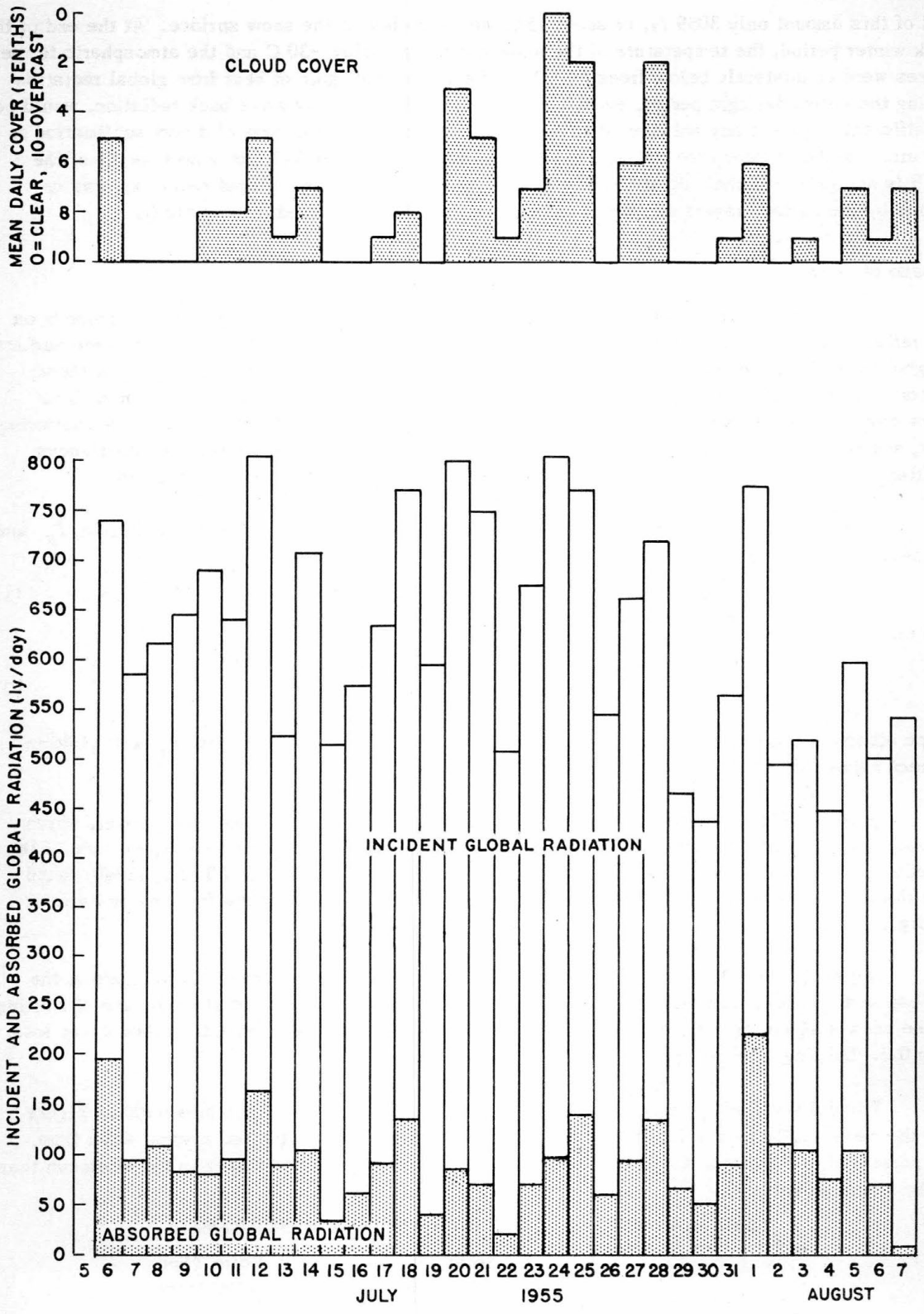

Figure 4. Daily radiation and cloud cover, Greenland Ice Cap, at 6800 ft msl, July-August, 1955. Total incident global radiation on snow cover, 6 July-7 August inclusive, was 20,628 langleys. Total global radiation absorbed by snow cover, 6 July-7 August inclusive, was 3059 langleys.

and of this amount only 3059 *ly*, or about 15%, was absorbed at the snow surface. At the end of the dark winter period, the temperature of the snow cover was below −30 C and the atmospheric temperatures were consistently below freezing. Therefore, the small gain of heat from global radiation during the entire daylight period, even if there were no loss by long-wave back radiation, would be insufficient to permit any ablation at this site, except for a minor amount of direct sublimation to the air. As shown later (see "Heat balance of snow cover," page 14), not more than 8% of the 3059 *ly* net gain in global radiation, or about 1% of the total incident global radiation, was retained by the surface layers of *snow* during the 33-day period covered by this study.

Albedo of snow.

6. The amount of incident solar radiation which is absorbed by a snow cover depends on the reflectivity or albedo of the snow surface. Some of the factors which affect albedo are surface roughness, melting, refreezing of melt water, and the presence of contaminants. Most of these factors are associated with the age of the snow surface since the time of the last storm. The snow cover in the central portions of the Greenland Ice Cap is not subject to melting or contamination, and because of continuous drifting the surface is always relatively new. The continuous drifting and erosion produce a patterned surface which does appear to affect the albedo.

The albedo, A, of a surface is defined as the ratio between the reflected radiation, I_R, and the incident radiation, I:

$$A = I_R / I \tag{1}$$

and the radiation absorbed by the snow cover, I_a, is:

$$I_a = I\,(1 - A). \tag{2}$$

Since albedo is not measured directly, errors in the observed values of I and I_R will yield incorrect values of A.

Hubley (1955) observed a diurnal variation in the albedo of a melting snow cover, which he ascribed in part to changes in sun angle. Eckel and Thams (1939) found no dependence of the albedo of the winter snow on solar altitude. In a later study, Prohaska and Thams (1940) found that the diurnal variation of albedo was largest with air temperatures above freezing and almost negligible with air temperatures below freezing.

During the period 6 July to 7 August 1955, when albedo measurements were made at the ice-cap site, air temperatures were always below 0 C and there was no visible evidence of melting at the snow surface. Skies were mostly cloudy; there were only 4 days with the cloud cover less than 0.5. Drifting or blowing snow occurred almost every day.

The daily values for albedo computed for all the hours of record are presented in Figure 5 and the mean hourly values for albedo under cloudy and clear skies, plotted against solar time, are presented in Figure 6. On both clear and cloudy days, albedo was higher in the afternoon than in the morning (Table I).

Table I. Mean Values of Albedo in the Morning and Afternoon

	Solar Time 0500-1100	Solar Time 1300-1900
Clear day	0.77	0.87
Cloudy day	0.80	0.86
All days of record	0.80	0.85

Note: On clear days, cloud cover was 0.2 or less, cloudy days had 0.7 or more cloud cover.

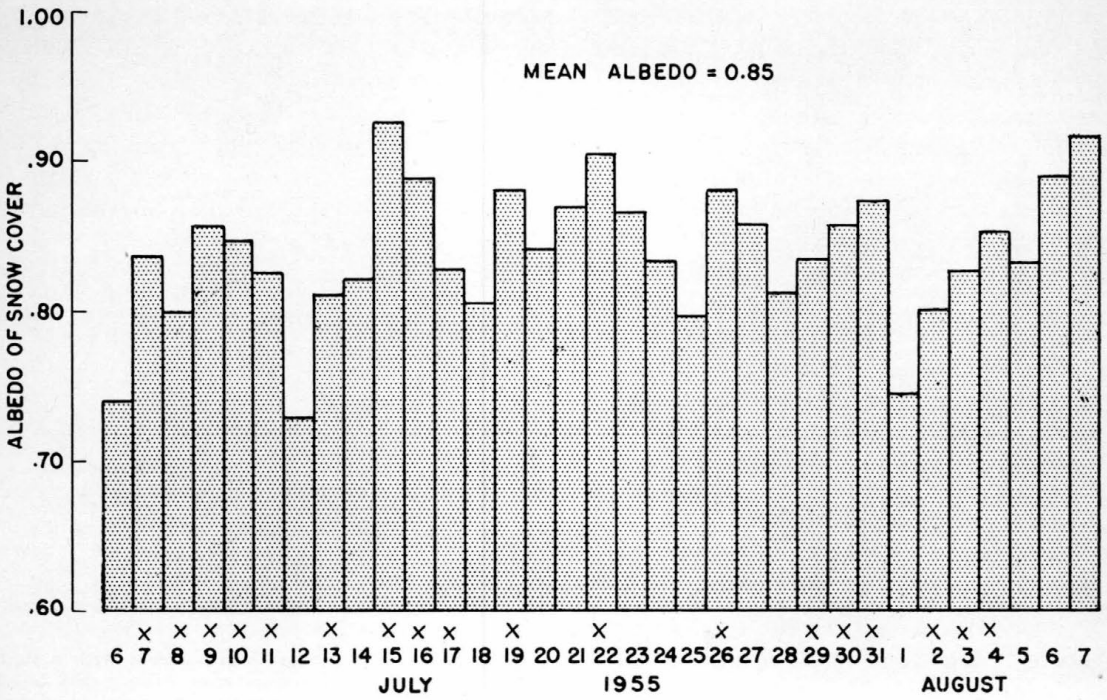

Figure 5. Daily albedo of snow cover, Greenland Ice Cap, at 6800 ft msl. Between 1000 and 1600 hr, 6 July-7 August, 1955. X = day on which snowfall occurred.

The difference may be due to reflections from the etched patterns on the snow surface, which were present more than 80% of the time during the period when the radiation measurements were made. The patterns are formed by wind erosion of the snow surface and frequently exhibit vertical or even undercut surfaces facing into the wind (Figs. 7-10). At the ice-cap site, the vertical surfaces faced toward the southeast, or into the morning sun.

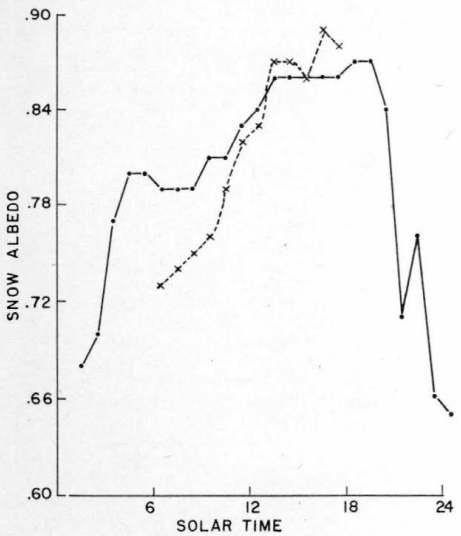

Figure 6. Variation of albedo with time, Greenland Ice Cap, 6800 ft msl.
. = Mean value for 30 days with more than 0.7 cloud cover.
× = Mean value for 3 days with less than 0.2 cloud cover.

The presence and orientation of erosional patterns on the snow surface may have sufficient effect on the albedo to require that specific measurements of reflected global radiation be made at each site where the precise determination of the energy balance is required. It appears also that the albedo of a permanent polar snow cover is much higher than that usually attributed to glacier snow and firn in the temperate zones.

Fluctuations in albedo which were recorded after 2100 and prior to 0500 hours, as shown in Figure 6, may be attributable in part to the instrumental problem involved in measuring the incident and reflected solar radiation at the low sun angles (of 3^{o}-18^{o}) during these periods.

Diffuse sky radiation.

7. Instantaneous measurements of diffuse sky radiation were made at frequent intervals by occulting the hemispherical pyrheliometer from direct solar radiation. The results are plotted in Figure 11. The diffuse sky radiation was also computed as follows: The solar radiation on a horizontal surface is

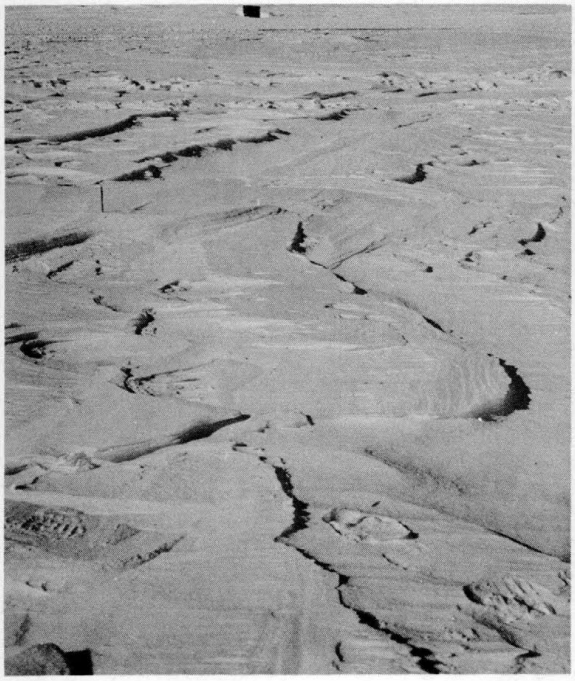

Figure 7. Patterns in a wind-slab snow surface which may have an orientation effect on albedo. Photographed at Resolute Bay, 74°41'N, 94°55'W.

Figure 8. Cuplike, wind-etched patterns with a superimposed drift of the barchan type. Albedo may be affected by directional reflection from the etched patterns, and by movement of the superimposed drifts past the pyrheliometer site. Photographed near the research site on the Greenland Ice Cap.

Figure 9. Variations in snow-surface patterns which may have a diurnal effect on albedo through change in sun angle and azimuth or by movement of the pattern as etching and filling takes place. Photographed near the research site on the Greenland Ice Cap.

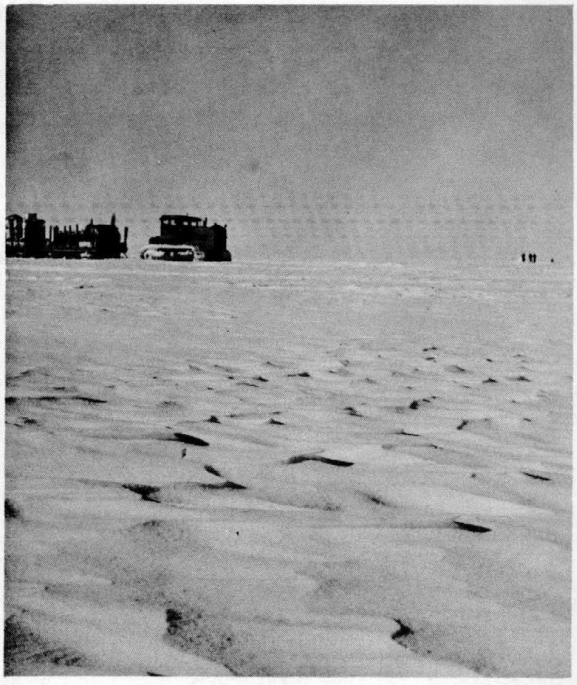

Figure 10. Sharply etched anvil-type drifts which may have a diurnal influence on albedo. Photographed near the research site on the Greenland Ice Cap.

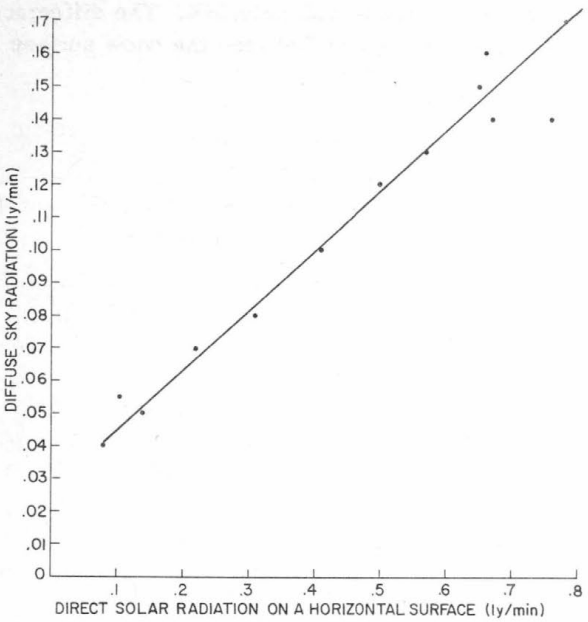

Figure 11. Diffuse sky radiation vs direct solar radiation, Greenland Ice Cap, 6800 ft msl.

computed from:

$$I_h = I_i \sin \phi \qquad (3)$$

where:

I_h = solar radiation on a horizontal surface

I_i = normal incidence solar radiation

ϕ = sun angle (above horizon).

The diffuse sky radiation is then computed from:

$$I_s = I_t - I_h \qquad (4)$$

where:

I_s = diffuse sky radiation

I_t = total global (solar and sky) radiation

I_h = solar radiation on horizontal surface.

Both measured and computed values are listed in Table II. Values are similar except for the period of low sun angle (less than 15°) after 1800 hr, when the measured values were larger than the computed values.

At the ice-cap site, diffuse sky radiation constituted 19% of the total incoming global radiation. In the temperate latitudes, sky radiation has been estimated to be 30 to 40% of the incoming global radiation (King, 1912).* The low percentage of diffuse sky radiation at the high-elevation Arctic site may be attributed to low atmospheric turbidity since, as Linke (1942)† has shown, the ratio of sky radiation to global radiation is small when the atmospheric turbidity is low.

Effect of clouds on radiation.

8. Observations of cloud cover were made every 3 hr during the period. Mean daily cloudiness plotted against daily incident global radiation (Fig. 12) shows that, even under full overcast conditions, large amounts of solar radiation were received at the snow surface. As shown in Table III, a mean cloud cover of 0.5 reduced the incident global radiation by only 6% and, even under conditions of full overcast, the snow surface received 65% as much global radiation as on a clear day. These high values for measured global radiation with overcast skies over a large snow field have been observed in the Antarctic also (Liljequist, 1953) and a relationship between cloud cover and global radiation similar to that shown in Figure 12 was obtained by Wallen (1949) from measurements made on the Karsa Glacier in Sweden.

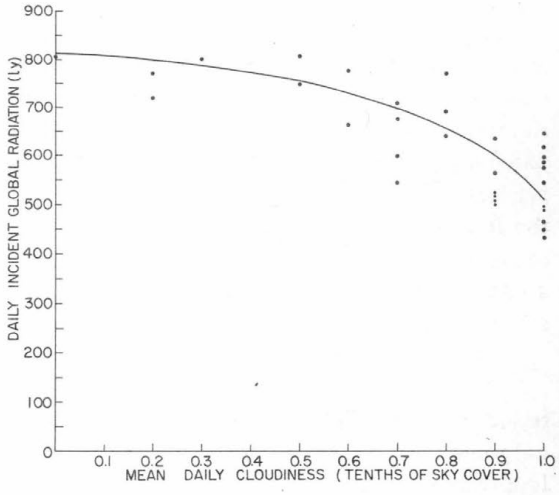

Figure 12. Daily incident global radiation vs mean daily cloudiness, Greenland Ice Cap, 6800 ft msl.

Kimball (1919) states that, under fully overcast conditions, there is an average decrease of 70% in global radiation received at the

* Cited in Sutton (1953).

† Cited in Fritz (1951, p 24).

earth's surface in the Temperate Zone. On the ice cap, the decrease was only 35%. The difference may be due to less dense clouds in the Arctic and to multiple reflection between the snow surface and the cloud base.

Table II. Computed and Measured Values for Diffuse Sky Radiation

1955	Time (hr)	Measured Sky Radiation (*ly*/min)	Computed Sky Radiation (*ly*/min)
27 July	1400	0.15	0.15
	1500	0.13	0.14
	1600	0.12	0.15
	1700	0.10	0.14
	1800	0.08	0.09
	1900	0.07	0.05
	2000	0.05	0.01
	2100	0.055	0.01
	2200	0.04	0
28 July	1200	0.14	0.14
	1400	0.16	0.13
1 August	1015	0.17	0.18

Table III. Incident Solar Radiation as a Function of Cloudiness

Mean Cloudiness	Radiation Received on a Horizontal Surface, in % of Clear-day Radiation
0	100
5/10	94
10/10	65

The relationship between global radiation received at the snow surface, the extent of cloud cover, and the elevation of the clouds is shown in Figure 13. It appears that low clouds were associated with a more complete cloud cover at this site. Although global radiation was reduced appreciably with extensive low cloud cover, it was still in excess of two-thirds of the amount received under clear sky conditions. The diffusion and reflection of large amounts of the incoming global radiation by an extensive cover of low clouds is the primary physical cause of that type of white-out on the ice cap in which depth perception is greatly reduced without a corresponding reduction in horizontal visibility. Some studies on this phenomenon are being incorporated in a separate report.

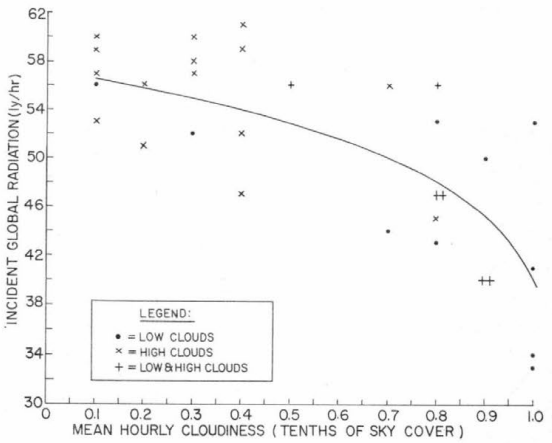

Figure 13. Effect of clouds on incident global radiation, Greenland Ice Cap, 6800 ft msl. 0930, 1230 observations.

As cloud cover increases, there is a large reduction in the heat loss from the snow surface by outgoing long-wave radiation. In Figure 14, the long-wave radiation balance, as computed from the measurements of net all-wave radiation and net global radiation, is plotted against mean daily cloud cover. Figure 15 shows the observed mean

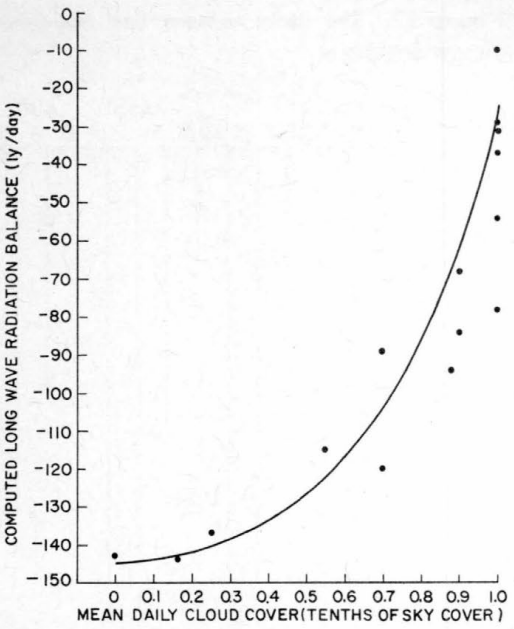

Figure 14. Computed long-wave radiation balance vs cloud cover, Greenland Ice Cap, 6800 ft msl.

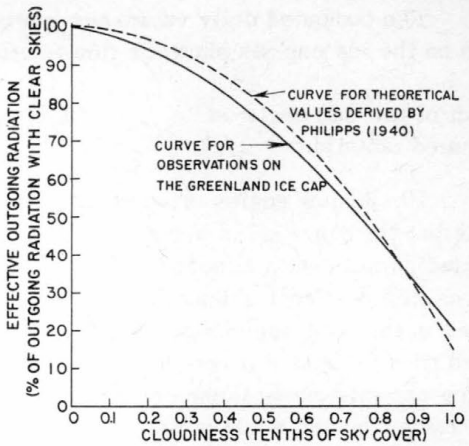

Figure 15. Effective outgoing radiation vs cloud cover, Greenland Ice Cap, 6800 ft msl.

decrease in effective outgoing radiation due to cloudiness, which compares favorably with the theoretical values derived by H. Philipps (1940). Since there is only a small decrease in incoming solar radiation with increasing cloud cover, the result is an increase in the net radiation balance (Fig. 16).

The net increase in all-wave radiation flux at the snow surface with increasing cloudiness indicates that, with similar atmospheric conditions, ablation would be greater at lower elevations and would extend to higher elevations during cloudy summers than during clear summers.

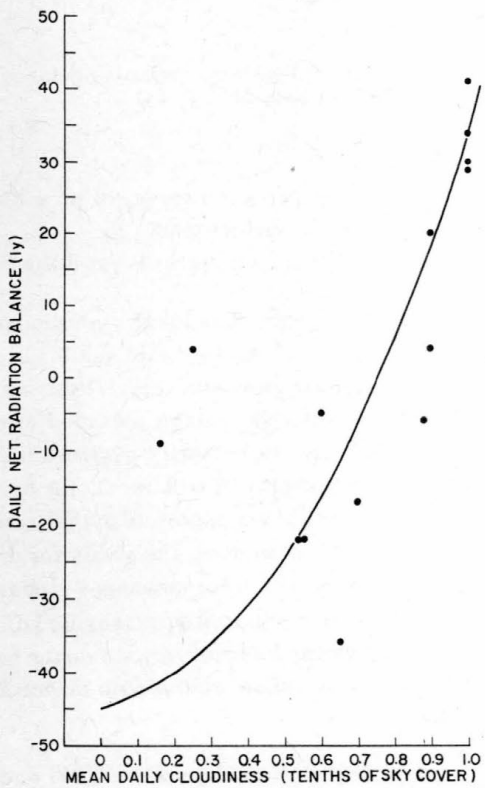

Figure 16. Net radiation balance vs cloud cover, Greenland Ice Cap, 6800 ft msl.

Atmospheric and terrestrial radiation.

9. Incoming and outgoing long-wave radiation was not measured directly, but was computed from measurements made with the net radiometer and the incident and reflected pyrheliometers. The long-wave radiation balance was computed from:

$$I_l - O_l = N - (I_s - O_s) \qquad (5)$$

where:

$I_l - O_l$ = long-wave radiation balance or effective outgoing radiation

I_l = incoming long-wave radiation from atmospheric water vapor and/or clouds

O_l = outgoing long-wave radiation from snow surface

N = net radiation balance

I_s = incoming solar radiation

O_s = reflected solar radiation

$I_s - O_s$ = solar radiation balance.

The computed daily values are plotted in Figure 17. The daily balance for long-wave radiation on the ice cap, as shown in this figure, is always negative.

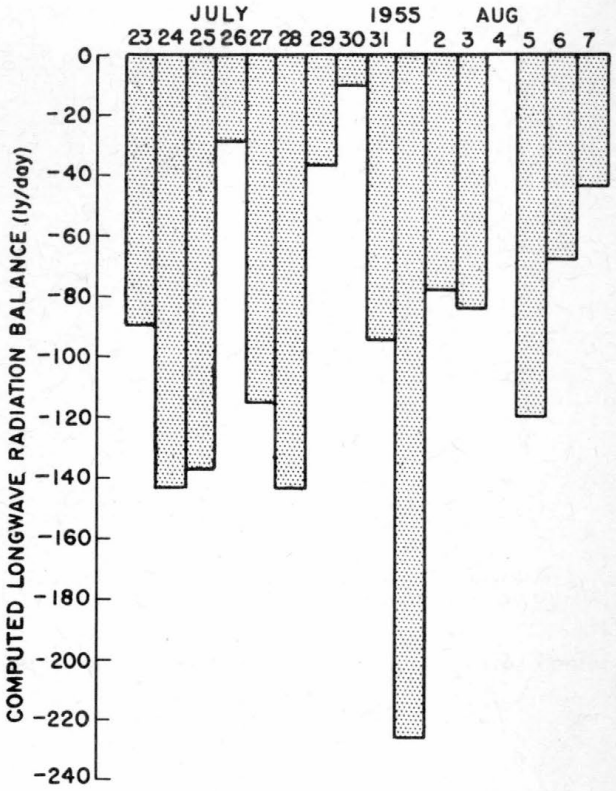

Figure 17. Computed daily long-wave radiation balance, Greenland Ice Cap, 6800 ft msl.

Effect of low sun angle on measured radiation.

10. At low angles of incident solar radiation, the response of hemispherically mounted pyrheliometers tends to diverge from the cosine law. Most solar radiation received in the polar regions during the summer comes from the sun at a very low angle. At the ice-cap site where these observations were made, the sun angle varies from a high of only 32° at solar noon in July, when these studies were started, to 6° at solar midnight in early August, when the observations were discontinued. Any appreciable divergence of the pyrheliometer from the theoretical cosine response at low sun angles would result in a large accumulative error in measured global radiation. The instrumentation and procedures used in these studies on radiation permitted evaluation of the effect of low sun angle on the response of the pyrheliometers.

From the equation:

$$I'_h = I_n \sin \phi \qquad (6)$$

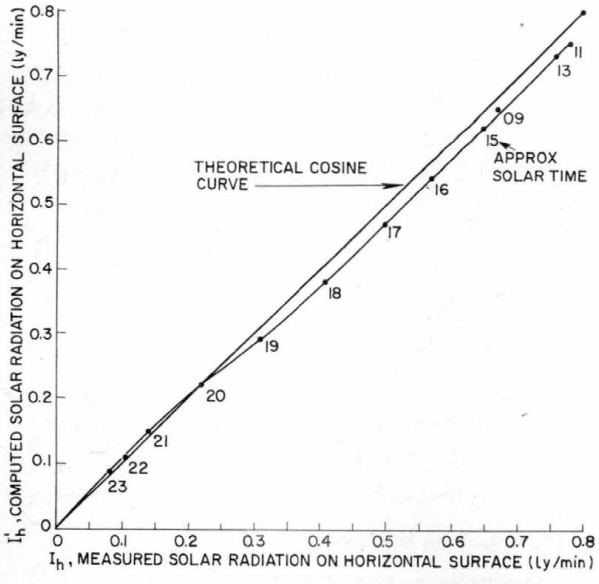

Figure 18. Incident solar radiation received on a horizontal surface, Greenland Ice Cap. Comparison of values measured with a hemispherical pyrheliometer and values computed from normal incident pyrheliometer measurements. Measurements made at 6800 ft msl.

where:

I'_h = solar radiation received on a horizontal surface and

I_n = solar radiation received on a normal surface,

the output of the normal incident pyrheliometer was converted to values for solar radiation receivable on a horizontal surface. These values were compared with the values obtained at the same time from the horizontally mounted hemispherical pyrheliometer. The direct solar radiation measured by the hemispherical pyrheliometer was obtained by subtracting the value for diffuse sky radiation from the total measured global radiation. Diffuse sky radiation was measured directly by occulting the sun for brief periods so the hemispherical pyrheliometer received no direct solar radiation.

The data obtained between 1200 and 2400 on one clear day are presented in Table IV and plotted in Figure 18. A mean positive error of 4%

Table IV. Effect of Sun Angle on Measured Incident Radiation

Approximate Solar Time	ϕ Sun Angle		Sin ϕ	I_n Measured	I_h Measured	I_h' Computed
	Degree	Minute				
2400	6	2	0.1045	0.85	0.08	0.09
2300	7	11	0.1248	0.92	0.10	0.11
2200	9	3	0.1564	0.98	0.14	0.15
2100	11	34	0.1994	1.09	0.22	0.22
2000	14	33	0.2504	1.17	0.31	0.29
1900	17	50	0.3062	1.24	0.41	0.38
1800	21	12	0.3611	1.30	0.50	0.47
1700	24	27	0.4147	1.31	0.57	0.54
1600	27	20	0.4592	1.35	0.65	0.62
1400	31	12	0.5175	1.41	0.76	0.73
1200	31	29	0.5225	1.44	0.78	0.75
				Total	4.52	4.35
				Mean	0.411	0.395
				Difference between means	0.016	
				Error	4.0%	

in measured global radiation is indicated for the period of the study.

For the 24-hr period within which these measurements were made, the measured total global radiation was 804 *ly*. The apparent error in the pyrheliometer record indicates that this measured global radiation was 32 *ly* higher than actually received on a horizontal surface. Within this apparent error attributed to divergence from a true cosine response, approximately 8 *ly* may be the product of temperature changes during the period, leaving a cosine response error for clear-day global radiation of about –3%.

It was not possible to determine whether a similar error might be present in the measurements of reflected radiation. It was observed that, at a very low sun angle, the inverted pyrheliometer appeared to respond to internal reflections of direct solar radiation on the glass globe. This observation is supported by the similar figures for incident and reflected radiation measured during the night hours (Tables AI and AII, Appendix). Since there were only 4 clear days, and average cloudiness exceeded 0.5 during the period of these investigations, and since albedo measurements appeared to include a similar error, no corrections were applied to the radiation data analyzed in other sections of this report.

Global radiation gradient.

11. Eppley pyrheliometers were installed at 5.7, 3.5, and 1.25 m above the snow surface to measure changes in solar radiation during arctic white-outs and blowing or falling snow. At the end of the season, the three pyrheliometers were checked against each other by exposing them at the same level for 5 hr. The difference in values obtained was used as a correction factor in comparing values when the instruments were mounted at different levels (Table V). The No. 1 pyrheliometer, located at 1.25 cm above the snow surface, was operated continuously during the season with the compensator on the recorder permanently set for the calibration constant of this instrument. To obtain measurements during periods of blowing snow, the middle (No. 2) and higher (No. 3) instruments were connected through an automatic step switch to the

Table V. Response of Three Hemispherical Pyrheliometers Exposed at the Same Elevation

Pyrheliometer Number		
1 (*ly*/min)	2 (*ly*/min)	3 (*ly*/min)
0.900	0.894	0.882

same recorder used for the No. 1 pyrheliometer. The recorded values were adjusted by the required amount, since it was not possible to make the necessary compensation in the recorder for all three pyrheliometers.

During periods of blowing snow the Eppley pyrheliometer mounted 1.25 m above the snow surface consistently recorded greater insolation than the pyrheliometers mounted at 3.5 and 5.7 m (Table VI). Nine separate instantaneous measurements made during periods of blowing snow

Table VI. Effect of Blowing Snow on Global Radiation Measured Near the Snow Surface

July 1955	Time (hr)	Elevation of Pyrheliometer above Snow Surface		Increase at Lower Level	
		5.7 m (*ly*/min)	1.25 m (*ly*/min)	(*ly*/min)	(%)
		Blowing-snow Storm			
7	1100	0.692	0.728	0.036	5.2
	1220	0.688	0.711	0.023	3.3
	1600	0.525	0.535	0.010	1.9
13	0830	0.570	0.585	0.015	2.6
	1230	0.614	0.652	0.038	6.2
16	1330	0.581	0.602	0.021	3.6
	1615	0.383	0.392	0.009	2.4
17	0845	0.664	0.697	0.033	5.0
22	0917	0.602	0.622	0.020	3.3
30	1115	0.620	0.639	0.019	3.1
	1130	0.652	0.674	0.022	3.4
	1145	0.661	0.683	0.022	3.3
	1200	0.609	0.615	0.006	1.0
	1215	0.570	0.574	0.004	0.7
	1230	0.541	0.558	0.017	3.0
	1245	0.516	0.534	0.018	3.5
	1300	0.504	0.519	0.015	3.0
	1315	0.483	0.495	0.012	2.5
	1330	0.462	0.471	0.009	2.0
		Clear, Calm Weather			
23	1030	0.941	0.942	+0.001	+0.1
24	1030	0.826	0.832	+0.006	+0.7
25	1145	0.959	0.948	−0.009	−0.9
	1315	0.884	0.877	−0.007	−0.8
	1530	0.680	0.681	+0.001	+0.2
	1615	0.595	0.586	−0.009	−1.5

Note: Measured density of blowing snow in the air on 30 July was 0.6 g/m^3 at approximately 1 m above the snow surface and 0.005 g/m^3 at 4 m.

between 7-22 July showed as much as 6% greater insolation at the lower levels than at 5.7 m. During a blowing-snow storm on 30 July, continuous records of global radiation at the three elevations were obtained over a period of several hours. The amount of radiation measured at 1.25 m was as much as 3.5% greater than that at 5.7 m. During this period, the amount of blowing snow in the atmosphere was measured at intervals with an instrument developed for the purpose (to be described in a later report covering the concurrent studies on drifting and blowing snow). The amount of blowing snow measured in the vicinity of the pyrheliometers was about 0.6 g/m^3 at 1 m and 0.005 g/m^3 at 4 m above the snow surface.

The solar radiation data presented in Table VI show that, without exception, solar radiation values during blowing-snow storm periods were higher close to the snow surface than at 5.7 m above the surface. An increase in measured radiation was observed also at 3.5 m, although of much lesser magnitude and less consistent. Radiation values selected at random from the record for several periods of clear weather (Table VI) show no difference between 1.25 and 5.7 m. The increase in radiation measured at the lower elevation during the periods of blowing snow may be due to multiple reflection within the layer of blowing snow.

Atmospheric transmission coefficient.

12. In passing through the earth's atmosphere, solar radiation is decreased in intensity by scattering due to air molecules and dust particles and absorption by water vapor. The solar radiation which finally reaches the earth's surface may be computed from:

$$I = \frac{I_o}{r^2} a^m \cos Z \qquad (7)$$

where:

I = total solar and sky radiation received on a horizontal surface at the ground, ly/min
I_o = total solar radiation received on a normal surface at the exterior of the atmosphere, ly/min
r = earth's radius vector
a = atmospheric transmission coefficient
m = solar air mass (ratio of length of actual path of solar beam to the path through the zenith)
Z = sun's zenith distance.

During the period of measurement, a cloudless day occurred on 24 July. From the Smithsonian Meteorological Tables (1951), I_o for that day was computed to be 2665 ly, and m for the ice-cap site was computed to be 2.8. The total measured global radiation on that day was 804 ly. Substituting these values in Equation 7, the atmospheric transmission coefficient was computed to be 0.968. The high value for the transmission coefficient indicates that the low value obtained for diffuse sky radiation at this site may be attributed to low atmospheric turbidity.

Heat balance of snow cover.

13. The upper layers of a snow cover receive heat: (1) from incoming global and long-wave radiation; (2) by conduction from the air if the air temperature increases with increase of height; (3) by heat of condensation if the vapor content of the air increases with increase of height; (4) by conduction from below if the temperature of the snow increases with increase of depth; and (5) by transfer of heat from precipitation which is warmer than the snow cover.

The upper snow layers lose heat (1) by outgoing long-wave radiation; (2) by conduction to the air if the air temperature decreases with increase of height; and (3) by conduction downwards if the snow temperature decreases with increase of depth.

Any surplus of heat which the upper snow layers receive may be used for melting or evaporation, or it may be conducted to lower layers if the snow temperature decreases with depth. For a column of snow in which melting does not occur, a change in the cold content (defined as the amount of heat required to raise a column of snow 1 cm^2 in cross section to 0 C) may be expressed as follows:

$$\Delta Q = I + R + Q_s + Q_a + F \tag{8}$$

where:

ΔQ = change in cold content, *ly* (positive for heat gain, negative for heat loss). Computed from,

$$Q = m\ t\ c \tag{8a}$$

where:

m = mass of snow, g
t = temperature of snow, °C
c = specific heat of snow, 0.5 cal/g – °C
I = incident global radiation – reflected global radiation
R = long-wave radiation balance (positive when incoming and negative when outgoing)
Q_s = amount of heat received from or lost to the snow, calculated from

$$Q_s = K\ dt/dz \tag{8b}$$

where:

$K = 0.0085\rho^2$ (ρ = density of snow)
dt/dz = temperature gradient in the snow
Q_a = amount of heat received from or lost to air
F = 680 M (latent heat of fusion × mass of sublimate, positive for condensation on the snow, negative for sublimation to the air).

The effective change in the heat balance of the snow cover at the ice-cap research site was computed from the snow cover studies and meteorological measurements made between 25 July-6 August inclusive, during which the most complete radiation measurements and snow profile records were obtained.

From snow profile measurements made on 25 July and again on 6 August, the change in cold content of the upper 70 cm of the snow cover was found to be –2 *ly*, which means that this portion of the snow cover gained 2 *ly*. Substitution of measured values for I, R, and Q_s in Equation 8 permitted computation of the combined values of $Q_a + F$. The results are shown in Table VII.

Table VII. Heat Balance of the Snow Cover at Site 2 for 13-day Period 25 July-6 August 1956

Gain (*ly*) Global Radiation (I) 1318	Loss (*ly*) Long Wave Radiation (R) 1195	Balance (*ly*) ($Q + Q_s + Q_a + F$) + 123
Distribution of heat gain, Equation 8		
Heat gain, top 70 cm snow (Q)	2 *ly*	
Heat gain, below 70 cm snow (Q_s)	96 *ly*	
Total gain for 13-day period ($Q + Q_s$)		98
Loss by transfer to air and by sublimation to air for 13-day period ($Q_a + F$)		25

Computation of separate values for Q_a and F was not possible because of the inability to obtain a precise measurement of the temperature of the snow surface. The mean temperature and dew point values for different elevations above the snow surface (Table VIII) show that there was a diurnal change in both the air temperature and the dew point. The increase in dew point accompanying the mid-day rise in air temperature indicates that sublimation from the snow cover to the air took place and probably accounts for most of the computed 25 *ly* loss from the snow cover by transfer to the air. The 123 *ly* potentially available to the snow cover was reduced by heat transfer to the air to a net gain of 98 *ly* for the 13-day period.

Table VIII. Mean Temperature and Dew Point at Different Levels
25 July to 6 August 1955

Time	Height above Surface (m)									
	Temperature (−°C)					Dew Point (−°C)				
	0.3	1.2	1.9	3.3	5.5	0.5	1.4	2.1	3.5	5.7
0100-0400	10.6	10.8	10.7	10.6	10.6	11.5	11.6	11.8	11.5	11.4
0500-0800	8.4	9.0	8.5	8.6	8.8	11.0	11.3	11.5	11.2	11.2
0900-1200	6.5	6.7	6.2	6.1	6.4	8.9	9.2	9.7	9.0	9.2
1300-1600	6.4	6.7	6.7	6.4	6.5	8.3	8.7	8.9	8.4	8.7
1700-2000	8.3	8.4	8.6	8.3	8.5	9.3	9.4	9.6	9.3	9.3
2100-2400	9.6	9.8	9.8	9.7	9.8	10.1	10.1	10.2	10.0	10.0

Using the seasonal duration of sunshine at 78° N. as a basis for computation, the 98-*ly* gain by the snow cover over 13 days extrapolates to a 1000-*ly* gain by the snow cover for the entire 260-day period when solar radiation may be available. This heat gain is sufficient to produce an integrated temperature rise of about 4.5 C in the snow profile extending down to the constant temperature isotherm of −24 C near 30 ft below the surface. Temperature measurements made by SIPRE parties in 1954 in pits at this site showed a 540-*ly* heat gain by the snow for a 56-day period between 28 June and 22 August, slightly more than half the amount computed as potential gain for the 260 days of possible sunshine in 1955.

For the 13-day period in 1955, there was a net heat balance of 7.6 *ly*/day. From the deep pit studies made in 1954, the average daily heat balance for a 56-day period was found to be 9.6 *ly*. The difference, although extremely small, may indicate an actual difference in the summer climate between the two years.

The extremely small supply of heat available to the central ice cap in Greenland is further emphasized when compared with the mean daily heat balance for a snow pack in the Sierra Nevada of California. Table IX shows comparative data for an altitude of about 7000 ft at each research

Table IX. Comparison of Mean Daily Heat Balance for a High Mountain Snow Pack in California and the High Ice Cap in Greenland

Heat Balance	Central Sierra Snow Laboratory California May-June 1952 (*ly*/day)	Site 2 Greenland July-August 1955 (*ly*/day)
Radiation, global and long-wave	+291	+9.5
Exchange between snow and air	+109	−1.9
Net daily gain	+400	+7.6

site and for approximately equal periods, although on opposite sides of the summer solstice. No uniform cover of snow exists at the Central Sierra Snow Laboratory after 1 June, and records from the ice-cap site were not available until after 5 July.

The difference between the net daily gain of 400 *ly* by the snow pack in the High Sierra and the 7.6-*ly* gain by the central Greenland Ice Cap during the period of approximate maximum radiational heat supply provides one explanation for the enormous climatological difference between two localities where snow is a major factor in the environment. In spite of an annual snowfall equivalent to 80 to 120 in. of water, the entire 10- to 20-ft-deep snow pack which accumulates each winter in the High Sierra is melted by early June. At the same elevation on the ice cap, the 5 to 10 water-equivalent inches of snow which fall each year remain to nourish the ice cap because of the unfavorable heat balance. The positive heat balance for an entire summer season on the ice cap is no more than that accumulated in 2-1/2 days in the Sierra. The apparent 2-*ly* difference in the daily heat budget between the 1954 and 1955 seasons on the ice cap is of negligible importance when compared with the 400-*ly* daily balance available to the high-mountain snow pack in the temperate zone.

Applied use of solar energy.

14. A silicon solar energy converter of the p-n junction type similar to those developed by the Bell Telephone Laboratories was tested at the ice-cap site. Measurements of the output of the solar cell, made under both clear and overcast skies, are plotted against the incoming solar radiation in Figure 19. The maximum output of the cell, 34 milliamperes, was obtained over a range of incoming global radiation values between 0.63-0.93 *ly*/min. The output was the same whether the cell was faced normal to the sun or normal to the horizon. This indicated that the cell was about as sensitive to radiation reflected from the snow surface as to direct global radiation and that maximum output was obtained at less than maximum solar radiation.

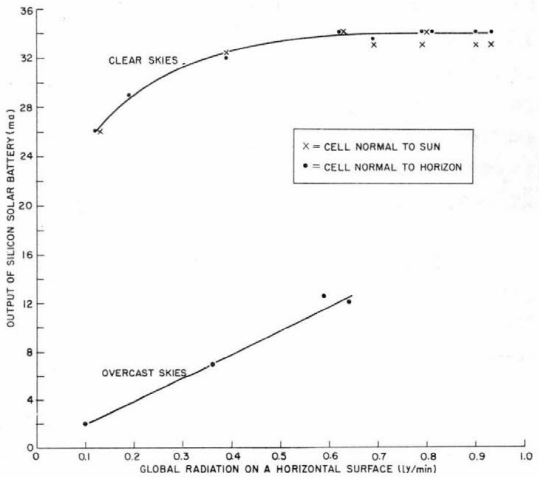

Figure 19. Output of silicon solar converter, Greenland Ice Cap, 6800 ft msl.

The output of the solar cell differs for clear and cloudy conditions even when exposed to the same intensity of global radiation (Fig. 19). This indicates that the cell has a higher output from global radiation received from a clear sky than for an equal intensity of global radiation received from overcast skies.

When the same instrument was tested at 42° N. latitude, the output was 27 ma for incoming global radiation of 1.4 *ly*/min. The higher output obtained in the Arctic may be due, in part, to greater efficiency at lower temperatures; in part, to a greater proportion of the global radiation at the ice-cap site being in the form of direct solar radiation; and, in part, to the low sun angle and high reflectivity of the snow surface, increasing the radiation available when the solar cell is faced normal to the sun's rays.

REFERENCES

Eckel, O., and Thams, Chr. (1939) "Untersuchungen uber Dichte, Temperatur, und Strahlungsverhältnisse der Schneedecke in Davos (Investigations on conditions of density, temperature, and radiation of the Davos snow cover)," in *Der Schnee und seine Metamorphose (Snow and its metamorphism)*, Beitrage zur Geologie der Schweiz, Geotechnische Serie, Hydrologie, Lieferung 3. Chapter V. p 273-340 (text in German). SIPRE Translation 14, 1954, p 245-304.

Fritz, Sigmund (1951) "Solar radiant energy and its modification by the earth and its atmosphere," in *Compendium of meteorology*. Boston: American Meteorological Society.

Hubley, Richard C. (1955) *Measurements of diurnal variations in snow albedo on Lemon Creek Glacier, Alaska,* Journal of Glaciology, no. 2, p 560-563.

Kimball, H. H. (1919) *Variations in the total and luminous solar radiation with geographical position in the United States,* Monthly Weather Review, November.

Liljequist, G. H. (1953) *Radiation and wind and temperature profiles over Antarctic snow-field – a preliminary note,* Proceedings of the Toronto Meteorological Conference 1953, Royal Meteorological Society.

Philipps, H. (1940) *Zur Theorie der Warmestrahlung in Bodennahe (Theory of heat radiation near the ground)*, Gerlands Beitrage zur Geophysik, Bd. 56, p 229-319 (text in German).

Prohaska, F., and Thams, Chr. (1940) *Neue Untersuchungen uber die Strahlungseigenschaften der Schneedecke (New research on the radiational properties of the snow cover)*, Helvetica Physica Acta, vol 13, p 21-44 (text in German).

Sutton, O. G. (1953) *Micrometeorology*. New York: McGraw-Hill Book Company, Inc.

Wallen, C. G. (1948-49) *Glacial-meteorological investigations on the Karsa Glacier in Swedish Lappland.* 1942-48, Geografiska Annaler.

APPENDIX

Table AI. Incident Solar Radiation (*ly*/hr)

1955	Time (hr)																							Total
	1	2	3	4	5	6	7	8	9	10	11	12	13	14	15	16	17	18	19	20	21	22	23	24	
July																									
6	8	11	13	17	23	28	37	54*	62	60	63	62	61	54	47	44	29	22	14	11*	6*	6	5	5	742
7	7	8*	13	17	19	25	35	36	40	45	43	43	40	38*	33	32	29	20	13	13	10	10	8	9	586
8	8	12	21	24	26	29	36	34	34	53	48	45	45	42	29	33	24	19	16	12	9	7	6	6	618
9	11	16	16	28	26	30	36	37	37	46	46	44	44	37	35	31	29	30	19	14	10	8	8	8	646
10	8	9	14	24	25	28	35	47	44	43	43	42	42	44	44	44	38	32	26	23	10	12	7	7	691
11	7	11	13	18	22	25	34	38	46	50	63	61	43	37	32	28	25	20	16	12	12	13	7	7	640
12	7	10	12	16	22	27	38	53	58	60	62	62	59	56	50	45	38	32	26	20	16	12	11	12	804
13	11	10	13	17	20	27	28	32	36	41	41	40	37	34	30	25	21	16	13	10	6	5	5	5	523
14	7	11	13	21	33	27	35	55	66	56	50	50*	47	45	39	34	31	25	21	12	7	10	7	6	708
15	6	6	13	15	20	26	29	39	36	33	36	38	33	39	31	27	22	15	14	11	10	6	5	5	515
16	8	10	18	17	19	29	31	45	38	38	44	49	43	36	32	29	23	20	13	10	7	6	5	5	575
17	6	9	11	19	19	25	26	36	40	57	58	44	47	38	36	31	25	23	25	25	14	8	7	7	636
18	8	10	13	19	28	27	38	51	57	56	63	62	58	55	49	44	35	31	26	12	9	9	6	5	771
19	7	11	21	15	22	28	35	36	39	52	45	41	50	40	34	26	23	18	13	10	7	5	5	11	594
20	12	14	23	26	31	38	47	51	51	59	61	59	56	50	48	42	31	26	21	16	13	10	8	7	800
21	10	13	18	21	29	34	44	49	53	57	38	53	53	53	48	38	33	26	22	16	12	10	9	9	748
22	10	13	14	15	20	24	30	33	34	38	39	40	39	32	31	26	21	15	11	8	5	4	3	3	508
23	4	7	9	13	18	25	34	40	44	53	60	59	57	53	48	38	26	18	19	16	11	7	5	8	672
24	11	15	21	25	30	37	44	50	55	58	60	59	56	53	48	42	36	27	22	15	12	10	9	9	804
25	11	14	19	24	30	37	44	50	55	58	59	58	56	52	47	41	36	36	11	9	6	5	4	7	769
26	4	10	10	14	18	25	28	35	37	43	41	45	43	40	39	30	23	16	12	9	7	6	4	6	545
27	6	10	11	19	20	37	32	36	38	40	49	59	47	44	46	40	34	26	20	15	11	8	7	8	663
28	9	13	17	22	28	35	41	47	52	55	56	56	53	50	46	40	33	25	17	6	5	5	4	4	719
29	4	5	7	9	19	26	27	37	38	40	37	36	34	31	31	24	16	15	10	6	5	3	2	3	465
30	4	5	9	12	17	19	25	34	32	32	39	40	34	30	26	22	17	13	9	5	4	3	3	3	437
31	4	6	9	11	17	26	29	38	38	47	52	46	44	42	43	31	23	18	16	8	5	4	4	4	565
Aug.																									
1	5	12	20	32	38	44	47	52	53	56	58	56	52	54	48	38	34	26	20	11	7	5	4	4	776
2	5	8	9	13	17	26	29	33	38	39	45	38	37	33	28	23	21	18	11	9	5	4	3	4	496
3	4	5	7	10	15	22	26	32	37	40	44	48	52	48	41	29	20	14	10	6	4	3	2	3	522
4	3	4	6	9	14	17	23	29	34	37	43	38	42	41	25	19	15	11	10	9	5	5	5	4	448
5	4	6	8	10	17	24	34	43	47	51	49	47	45	36	38	36	25	23	16	11	7	5	8	7	597
6	3	8	10	10	13	19	25	31	38	40	51	48	47	43	38	26	20	12	7	5	2	2	2	2	502
7	4	5	7	11	9	14	22	31	40	49	50	50	49	45	40	26	28	17	17	9	5	7	5	3	543
8	6	12	14	16	28	36	34																		163

* Estimated.

Table AII. Reflected Solar Radiation (*ly*/hr)

1955	Time (hr)																							Total
	1	2	3	4	5	6	7	8	9	10	11	12	13	14	15	16	17	18	19	20	21	22	23	24	
July																									
6	7	8	10	13	17	22	26*	33*	38	40	43	43	41	37	32	32	20	17	11	9	6	5	5	5	520
7	4	6	9	13	16	21	29	30	33	37	36	36	34	32	28	27	25	17	13	11	10	10	8	8	493
8	7	8	17	20	23	23	29	28	27	41	40	37	36	31	25	28	21	17	13	11	9	7	7	6	511
9	7	13	12	21	24	26	31	31	31	39	39	38	38	33	29	27	26	28	17	13	10	10	10	10	563
10	8	9	11	22	24	28	32	38	37	36	36	36	36	36	37	40	34	31	25	22	10	10	7	6	611
11	6	8	10	15	18	20	28	31	37	41	50	49	36	35	28	25	23	18	15	13	13	12	8	7*	546
12	7	8	10	13	16	21	29	37	39	42	45	46	46	43	40	37	32	28	25	20	17	14	13	13	641
13	11	8	9	11	14	20	22	25	28	32	33	33	32	28	25	21	20	16	13	11	7	6	5	5	435
14	5	7	9	14	24	23	29	38	44	41	44	48	46	42	40	37	32	27	22	10	5	7	6	5	605
15	5	10	10	11	17	25	29	33	33	31	34	38	30	36	29	26	20	16	13	11	10	7	4	4	482
16	5	8	17	16	18	25	29	42	37	38	37	40	35	31	27	25	21	17	12	10	8	7	5	5	515
17	5	6	8	16	16	21	23	29	31	47	48	37	41	32	32	27	23	22	23	23	14	8	7	6	545
18	6	7	10	14	22	22	30	40	44	46	50	50	48	46	41	37	31	29	22	11	8	9	7	6	636
19	6	10	20	14	18	26	36	37	32	44	38	36	44	36	30	26	21	18	14	12	10	8	7	11	554
20	10	16	21	23	26	26	34	40	43	47	49	50	49	47	42	38	31	27	24	20	17	14	11	9	714
21	10	13	16	19	24	26	33	38	41	45	48	46	46	45	42	33	30	26	24	20	16	14	13	12	680
22	12	13	14	14	17	21	28	29	31	34	35	36	36	30	28	25	21	16	13	10	8	7	5	5	488
23	5	7	8	12	16	22	28	34	38	44	50	51	51	48	44	38	24	17	19	16	11	6	5	8	602
24	10	13	16	20	24	28	33	38	43	47	50	50	50	47	43	40	34	28	23	19	15	13	11	11	706
25	11	12	16	20	24	27	32	37	41	45	47	48	47	44	40	37	31	29	10	8	7	5	5	5	628
26	5	9	9	12	16	22	24	30	32	37	36	40	38	37	36	25	19	15	11	10	7	6	5	5	486
27	5	8	10	16	16	26	26	31	33	34	49	43	38	40	38	34	28	23	19	15	12	10	8	8	570
28	8	10	14	17	22	25	30	36	39	43	46	46	46	43	38	33	28	22	16	6	4	4	4	4	584
29	3	4	10	7	18	22	22	29	28	32	32	32	30	28	25	20	13	13	8	7	6	4	4	2	399
30	3	4	7	11	14	16	22	28	28	28	34	34	29	25	23	19	17	13	10	6	5	4	3	3	386
31	4	4	7	10	14	23	25	33	32	40	46	43	37	37	40	28	18	14	11	5	2	2	1	1	477
Aug.																									
1	1	7	13	20	25	23	31	33	39	41	44	44	41	41	38	32	26	22	17	7	4	3	2	1	555
2	2	5	6	8	13	20	22	25	29	32	36	31	31	27	23	19	16	13	8	7	4	3	2	2	384
3	2	2	5	7	11	17	20	25	29	32	35	42	45	41	35	22	16	11	8	5	4	2	1	1	418
4	1	2	4	6	12	15	20	24	28	31	37	31	37	37	21	16	13	10	8	7	4	4	4	2	374
5	1	2	5	7	11	17	25	34	37	42	40	41	40	30	32	36	20	20	16	10	8	7	7	6	494
6	2	2	5	6	5	10	11	25	33	34	46	44	44	40	35	25	18	13	9	7	5	4	4	4	431
7	4	6	7	14	13	18	29	35	38	41	43	45	44	41	37	26	28	17	18	11	5	6	5	5	536
8	5	11	14	19	19	28	36	34																	166

* Estimated.

APPENDIX (Continued)

Table AIII. Net All-Wave Radiation (*ly*/hr)

1955	Time (hr)																							Total
	1	2	3	4	5	6	7	8	9	10	11	12	13	14	15	16	17	18	19	20	21	22	23	24	
July																								
23	0	0	0	0	1.0	1.0	1.9	3.8	4.7	4.7	2.8	1.0	−1.0	−3.8	−5.6	−2.8	0	0	−6.6	−5.6	−2.8	−1.9	−3.8	−3.8	−16.8
24	−3.8	−2.8	−1.9	−1.0	1.0	5.6*	3.8	4.7	4.7	4.7	3.8	1.9	−0.9	−2.8	−5.6	−6.6	−7.5	−7.5	−7.5	−6.6	−5.6	−5.6	−4.7	−4.7	−44.9
25	−3.8	−3.8	−3.8	−1.9	0	6.6*	3.8	5.6	5.6	5.6	4.7	1.9	0	−1.9	−4.7	−6.6	−4.7	0.9	0	0	0.9	0	0	0	+4.4
26																2.8	1.9	0.9	0.9	0.9	0	0	0	0.9	+30.0**
27	0	0	0	1.9	2.8	4.7	4.7	3.8	3.8	3.8	3.8	3.8	0.9	−2.8	−4.7	−6.6	−6.6	−6.6	−5.6	−5.6	−5.6	−4.7	−3.8	−3.8	−22.4
28	−2.8	−1.9	−1.9	0	0.9	2.8	4.7	5.6	4.7	4.7	2.8	0.9	−0.9	−2.8	−3.8	−5.6	−6.6	−6.6	−5.6	0	0.9	0.9	0.9	0	−8.7
29	−2.8	0.9	0.9	0.9	−0.9	1.9	2.8	3.8	2.8	2.8	1.9	1.9	1.9	2.8	1.9	1.9	0.9	0.9	0.9	0	0	0	0	0.9	+29.0
30	0	0.9	0.9	0.9	1.9	1.9	1.9	2.8	2.8	2.8	2.8	4.7	3.8	3.8	2.8	2.8	0.9	0.9	0.9	0	0	0.9	0	0	+41.1
31	−0.9	0	0.9	0.9	0.9	0.9	0	2.8	2.8	0.9	−1.9	−2.8	0.9	−0.9	−3.8	−1.9	0	0.9	0	−0.9	−1.9	−0.9	−0.9	−0.9	−5.8
Aug.																								
1	−1.9	0	−4.7	−3.8	−0.9	3.8†	3.8†	3.6†	3.8	4.7	3.8	1.9	1.9	0.9	−3.8	−3.8	−4.7	−5.6	−5.6	−0.9	2.8	0	0	0	−4.7
2	0.9	1.9	0.9	2.8	2.8	1.9	1.9	1.9	1.9	2.8	3.8	2.8	2.8	1.9	0.9	0.9	0.9	0	0	0.9	0.9	0	−0.9	−0.9	+33.7
3	0.9	0.9	0.9	0.9	1.9	2.8	2.8	2.8	3.8	3.8	2.8	0.9	−2.8	−3.8	−4.7	0	1.9	0.9	0.9	0	0	0	0.9	0	+19.5
4	0.9	0.9	0	0.9	2.8	1.9	2.8	0.9	2.8	2.8	2.8	0.9	0.9	1.9	0.9	0.9	0.9	0.9	0	−0.9	−1.9	−1.9	−0.9	−0.9	+20.3
5	0	0.9	1.9	1.9	2.8	2.8	2.8	3.8	3.8	4.7	1.9	0.9	0	−0.9	−1.9	−4.7	−5.6	−6.6	−6.6	−5.6	−5.6	−4.7	−1.9	−0.9	−16.8
6	−1.9	−1.9	−0.9	−0.9	0.9	1.9	1.9	2.8	3.8	4.7	2.8	1.9	−1.9	−3.8	−3.8	−3.8	1.8	0.9	0.9	0	0	0	−0.9	0	+4.5

* Possible increase due to reflection.

† Estimated, blowers blocked.

** Estimated.